

## TIBER-II TF WINDING PACK DESIGN

J. A. Kerns, J. R. Miller, D. S. Slack, and L. T. Summers

Lawrence Livermore National Laboratory  
University of California  
P.O. Box 5511, L-643  
Livermore, CA 94550

UCRL--96862  
DB88 004408

### Abstract

The superconducting, toroidal-field (TF) coils in the Tokamak Ignition/Burn Engineering Reactor (TIBER II) are designed with cable-in-conduit conductor (CICC) using Nb<sub>3</sub>Sn composite strands. To design the CICC winding pack, we used an optimization technique that maximizes the conductor stability without violating the constraints imposed by the structure, electrical insulation, quench protection, and fabrication technique. Detailed helium-properties codes calculate the heat removal along a flow path, and detailed field calculations determine the temperature, current, and stability margins. The conductor sheath is designed as distributed structure to partially support the combined in-plane and out-of-plane loads generated within the winding pack. Pancakes of the coil are wound, reacted, and insulated before being potted in the case. This design is aggressive but fully consistent with good engineering practice.

### Introduction

The TIBER II TF superconducting coils are designed to operate at steady state, with a current density of approximately 40 A/mm<sup>2</sup> at 12 T and a total nuclear heat load of 72 kW. This performance level can be attained with CICC windings that also provide a high level of stability. The CICC comprises a cable of multifilamentary composite strands in a strong steel sheath. The sheath around the cable provides a channel for helium flow, and it reacts against the vertical, centering, and out-of-plane loads that are electromagnetically-generated in the TF inboard leg.

The CICC design is specific to the required magnetic field and the thermal, mechanical, and geometric constraints determined by the TIBER design. The conductor design process was described by Miller and Kerns [1]. In this process, a point conductor design is developed from general requirements; then the coil is designed so the conductor design can be evaluated under the operating thermal and mechanical loads. This process is reiterated as necessary to obtain the optimum coil and conductor designs (cf. Fig. 1 of Ref. 1). The resulting TIBER II TF conductor design is presented here, with a discussion of its design considerations.

### Method

Table 1 lists operating parameters of a TF coil in this design. The list is the result of several design iterations. Several of the choices, such as  $I_{op}$  and  $V_D$ , are based on judgments of fabricability, practicality, reliability, etc. Other parameters, such as the maximum field and stored energy, result from the reactor design guidelines for TIBER II. In designing the conductor, we focused on attaining the highest winding-pack current density subject to limits by stresses, coil protection, and heat removal. Conductor parameters are determined by optimizing the conductor stability as described in Ref. [1]. The parameters satisfying the TIBER II TF coil design are given in Table 2.

A critical part of the optimization process is determining the total strain in the superconducting filaments. Strain results from differential cooldown contraction and generated electromagnetic forces. Control of electromagnetic forces is the most difficult in the straight leg of the TF coil where space is limited. The conductor design reflects measures taken to handle the loads in that region: including the vertical separating loads, the radial inward or centering loads, and the toroidal overturning loads

Table 1. Operating parameters for the TIBER II toroidal-field coil.

Description	Symbol	Value
Magnetic field	$B_{max}$	12 T
Operating current	$I_{op}$	36 kA
Winding-pack current density	$J_{pack}$	40 A/mm <sup>2</sup>
Stored energy	$E_s$	380 MJ
Coil dump voltage	$V_D$	10 kV
Estimated maximum hot spot temperature	$T_{max}$	130 K
Estimated maximum quench pressure	$P_{max}$	40 MPa
Helium inlet temperature	$T_{in}$	4.5 K
Average length of one turn	$L_T$	18.55 m

Table 2. Conductor design parameters for the TIBER II toroidal-field coil.

Effective area of a turn, $A_{eff}$	904 mm <sup>2</sup>
Conductor + insulation size	26.9 x 33.6 mm
Insulation thickness	0.5 mm
Conductor, cable-space cross section	510 mm <sup>2</sup>
Fraction of conductor in the cable space	0.60
Fraction of copper in the conductor	0.60
Cable pattern	5 x 5 x 5 x 3
Strand diameter	1.02 mm
Overall, winding-pack materials fractions	
$f_{steel}$	0.37
$f_{insulation}$	0.06
$f_{conductor}$	0.34
$f_{He}$	0.23
Sheath material	JBK-75

MASTER

28

that arise from  $J \times B$  forces generated by the poloidal field (PF) and plasma magnetic fields interacting with TF currents. In the inboard leg, the load is tensile and parallel to the conductor axis, while the latter two loads are compressive and transverse to the conductor axis. Once structural steel is appropriately added to the outside of the CICC to control these loads, then the state of strain in the superconducting filaments can be estimated [1-3].

In the inboard leg, we assume that the vertical separating force in the coil case and that in the winding pack sheath, i.e. both the distributed steel and the steel in the case, are equally stressed. Thus, we can estimate the strain in the sheath. Preliminary experiments were performed using these two forces to estimate the initial filament strain in a CICC and to determine the relationship between the sheath strain and the filament strain under electromagnetic loads. From the results of these experiments, an empirical relation has been constructed to predict the operating filament strain [1].

In early iterations of the TF design, it is difficult to have all the winding-pack stresses clearly determined. Certainly, the out-of-plane loads are not as well determined as the vertical and centering loads until the machine design is quite advanced. Thus, it is necessary to provide adequate distributed structure to combine these loads. We handle this uncertainty in the optimization procedure by limiting the allowable tensile stress in the conductor sheath to about one-third of yield, whereas our minimum static allowable is that the von Mises equivalent stress in the sheath be less than two-thirds the yield or one-half the ultimate stress.

When the conductor point design has been completed, we proceed with detailed helium-flow and conductor stress analyses. The point design is initially based on an estimate of the helium temperature in the CICC, but the temperature along the flow path through the 260-m-long TF coil can be calculated after the conductor and coil configuration are defined. The flow analysis and calculation of temperature margin along a conductor are complicated because the magnetic field and the nuclear heating around the TF coil vary as a function of poloidal angle  $\theta$  (Fig. 1) and of depth into the coil. Details of the

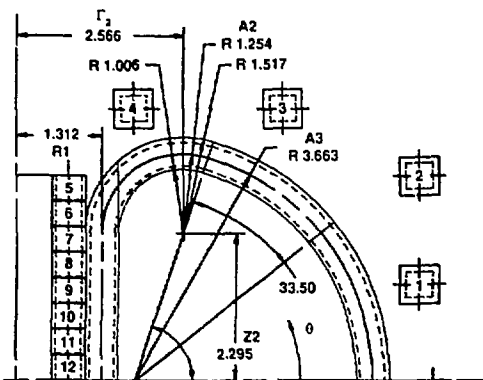


Fig. 1. Section view of TIBER II toroidal-field and poloidal-field coil set. The poloidal angle ( $\theta$ ) is measured from the midplane about the plasma axis.

variation of the helium properties along the flow path are included in the analysis and margins in current, temperature, and stability [4] have been calculated for a variety of heat loads and flow conditions.

A study of outlet pressure as a function of mass flow rate for varying inlet pressures with a 72-kW nuclear heat load is shown in Fig. 2. The helium inlet and outlet pressures and temperatures are chosen so that the stability margin ( $\Delta H$ ) at any location along the flow path is greater than or equal to the design limit of  $300 \text{ mJ/cm}^3$ . We have chosen inlet conditions of  $2.1 \text{ MPa}$  at  $4.5 \text{ K}$  and a total mass flow rate of  $3.8 \text{ kg/s}$  ( $0.02 \text{ kg/s per channel}$ ) for the TF coil system. Figure 3 shows the calculated stability margin along the conductor for these conditions.

The oscillatory nature of this curve occurs because  $B$  varies in the windings from the inboard region to the outboard region in the TF coil. The magnitudes of  $\Delta H$  increase since  $B$  decreases toward zero with depth into the windings. We have chosen to pancake wind the TF coils and inject helium at the inner crossover turn on the outboard leg; therefore, helium flows toroidally around the coil outward from the plasma axis. Thus, the high field turns receive the coldest helium. The inner turns are also exposed to the highest nuclear heat loads, especially on the inboard leg. It is apparent in Fig. 3 that the oscillations of  $\Delta H$  are superposed on an initially decreasing trend, which results from the high heat in the inner turns. Deeper into the winding, the heat load decreases and  $\Delta H$  generally increases; because the current-sharing temperature increases faster (with decreasing  $B$ ) than the helium temperature increases. In fact, far enough along the flow path the helium temperature decreases because expansion cooling exceeds the nuclear heating.

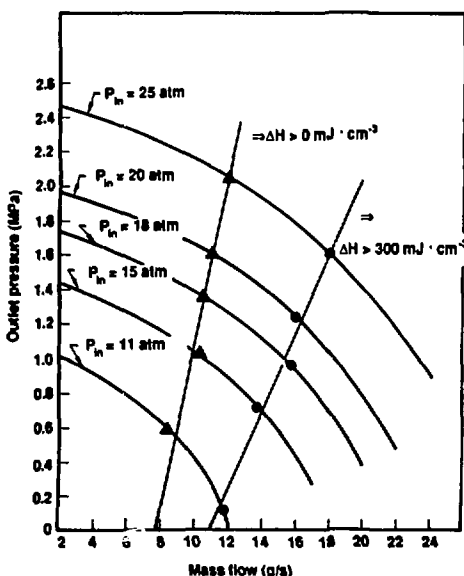


Fig. 2. Helium outlet pressure as a function of mass flow rate for inlet pressures from  $1.11$  to  $2.53 \text{ MPa}$ .

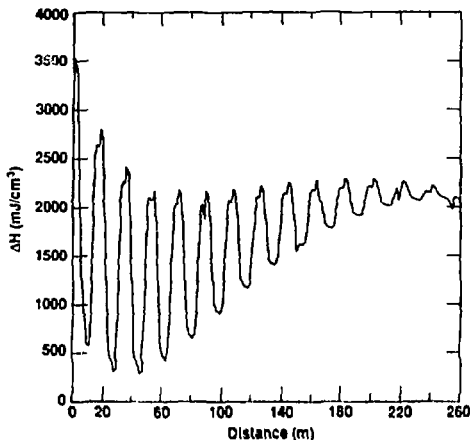


Fig. 3. Flow analysis of the toroidal-field conductor in which the stability margin is plotted as a function of distance along the flow path. Total heat input is 72 kW.

As the machine design nears completion an accurate determination of the mechanical loads in the winding pack is possible. Figure 4 shows the final design of the CICC for the TIBER II TF coils including its structural channel pressed over the helium containment sheath. Also indicated are the tensile stress in the sheath and channel, the compressive stress in the legs of the channel, and the compressive stress in the web joining the legs [5]. These are the maximum values from each type load and are not imposed uniformly over the winding pack. There are, however, small regions near the top and bottom of the straight inboard leg where values nearly equal to these are attained simultaneously. Note that the legs are subjected only to a combination of centering and vertical loads while the web is stressed only by the out-of-plane and vertical loads. The highest average von Mises equivalent stress is in the legs (580 MPa), which is well below two-thirds the yield for JBK-F5 steel (800 MPa).

#### Conclusions

The TIBER II TF coils have been designed using a procedure that optimizes conductor performance at the high fields and high current densities required. Detailed heat removal and calculations show the TIBER II TF system capable of accepting 72 kW while retaining adequate stability margin. It has also been verified that the stress levels in the sheath and structural channel as a result of mechanical loads in the TF inboard leg are not excessive.

#### Acknowledgments

This work was performed under the auspices of the U.S. Department of Energy by Lawrence Livermore National Laboratory under Contract W-7405-Eng-4B.

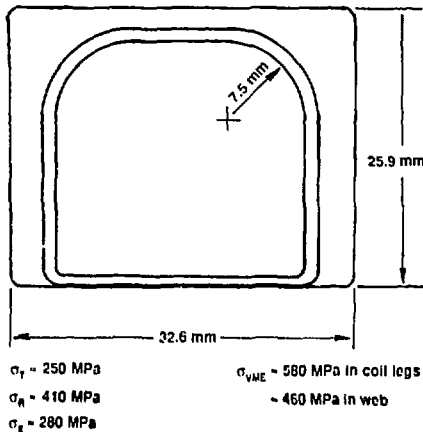


Fig. 4. Sheath design for TIBER II toroidal-field coils. The conductor is surrounded by a thin conduit, sized to quench-pressure approximations. The thick structural member is designed to react against the tension ( $\sigma_T$ ), radial ( $\sigma_R$ ), and overturning stresses ( $\sigma_x$ ).

#### References

- [1] J. R. Miller and J. A. Kerns, "Cable-in-Conduit Conductor Optimization for Fusion Magnet Applications," presented at the 12th Symposium on Fusion Engineering, Monterey, CA, Oct. 12-15, 1987.
- [2] J. R. Miller, M. R. Chaplin, L. T. Summers, M. M. Steeves, and M. O. Hoenig, "The Initial Filament Strain State of Cable-in-Conduit Superconductors and the Relation of This Strain to Large-Bore, High-Field Magnet Design," presented at the Applied Superconductivity Conference, Baltimore, MD, September 1986.
- [3] J. R. Miller, J. P. Zbasnik, L. T. Summers, and M. R. Chaplin, Investigations of Cable-Sheath Interactions in Cable-in-Conduit Superconductors, Lawrence Livermore National Laboratory, Livermore, CA UCRL-96000 (1987).
- [4] J. A. Kerns, D. S. Slack, and J. R. Miller, "Thermal Analysis of the Forced-Cooled Conductor for the TF Superconducting Coils in the TIBER-II ETR Design," presented at the CEC/ICMC, St. Charles, IL, June 1987.
- [5] J.D. Lee, Ed., TIBER II/ETR Final Design Report, Lawrence Livermore National Laboratory, Livermore, CA UCID-21150 (in press).

#### DISCLAIMER

This report was prepared as an account of work sponsored by an agency of the United States Government. Neither the United States Government nor any agency thereof, nor any of their employees, makes any warranty, express or implied, or assumes any legal liability or responsibility for the accuracy, completeness, or usefulness of any information, apparatus, product, or process disclosed, or represents that its use would not infringe privately owned rights. Reference herein to any specific commercial product, process, or service by trade name, trademark, manufacturer, or otherwise does not necessarily constitute or imply its endorsement, recommendation, or favoring by the United States Government or any agency thereof. The views and opinions of authors expressed herein do not necessarily state or reflect those of the United States Government or any agency thereof.